JACS
JOURNAL OF THE AMERICAN CHEMICAL SOCIETY

Article

pubs.acs.org/JACS

A Simple Approach for Predicting the Spin State of Homoleptic Fe(II) Tris-diimine Complexes

Hoa Phan,[†,∥] Jeremy J. Hrudka,[†] Dilyara Igimbayeva,[‡] Latévi M. Lawson Daku,[§] and Michael Shatruk*[,†]

[†]Department of Chemistry and Biochemistry, Florida State University, 95 Chieftan Way, Tallahassee, Florida 32306, United States
[‡]Department of Chemistry, L. N. Gumilyov Eurasian National University, 5 Munaitpasov Street, 010008 Astana, Kazakhstan
[§]Department of Physical Chemistry, University of Geneva, 30 Quai Ernest-Ansermet, CH-1211 Geneva 4, Switzerland

Supporting Information

ABSTRACT: We propose a simple method for predicting the spin state of homoleptic complexes of the Fe(II) d^6 ion with chelating diimine ligands. The approach is based on the analysis of a single metric parameter within a free (non-coordinated) ligand: the interatomic separation between the N-donor metal-binding sites. An extensive analysis of existing complexes allows the determination of critical N···N distances that dictate the regions of stability for the high-spin and low-spin complexes, as well as the intermediate range in which the magnetic bistability (spin crossover) can be observed. The prediction has been tested on several complexes that demonstrate the validity of our method.

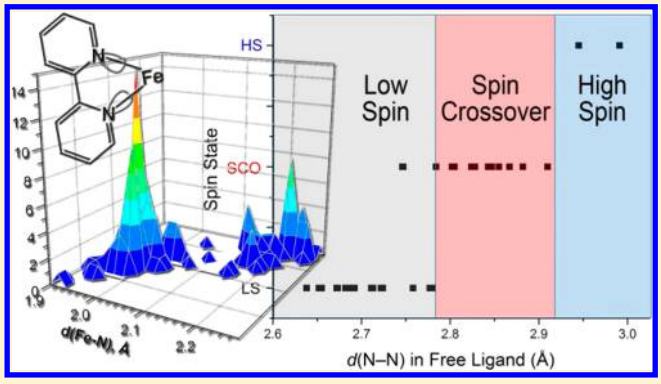

INTRODUCTION

After the initial discovery in 1930s, spin crossover (SCO) has become one of the most studied phenomena associated with molecular bistability.[1] Although the switching between the low-spin (LS) and high-spin (HS) electronic configurations has been observed in many complexes of d^4–d^7 transition metal ions, the Fe(II) complexes account for more than 90% of known SCO materials.[2] Most commonly, the coordination environment around the Fe(II) ion in such complexes consists of six N-donor atoms that provide an intermediate ligand field for occurrence of the SCO.[3] The spin transition itself can be driven by changes in temperature, pressure, or light irradiation.[4]

Despite the numerous studies on Fe(II) SCO complexes, predicting the occurrence and temperature of the spin-state conversion remains a nontrivial task. The SCO behavior can be extremely sensitive not only to the first coordination sphere around the metal ion but also to more subtle crystal packing effects. The quantum–chemical calculations, which have become a powerful tool for coordination chemists in recent decades, still encounter significant problems in predicting the possibility of the LS↔HS conversion due to the necessity to deal with the open-shell system and the relatively small energy difference between the LS and HS states.[5]

Given the general interest in magnetically bistable molecular materials, it is not surprising that simpler approaches were sought to provide a more reliable guide to the design of new SCO complexes. Thus, Busch et al. suggested to evaluate the possibility of SCO in an octahedral Fe(II) complex by studying the ligand field splitting ($10Dq$) of a Ni(II) complex with the same set of ligands.[6] The $10Dq$ value can be easily estimated from the first spin-allowed d-d transition ($^3A_{2g} \rightarrow {}^3T_{2g}$) in the optical absorption spectrum of the Ni(II) complex. It was shown that the values of $10Dq$ in the range of 11 200–12 400 cm^{-1} often led to the observation of the SCO in the corresponding Fe(II) complexes. Such an approach, while simple, still requires the preparation of the Ni(II) analogue, the measurement of its optical spectrum, and the "leap of faith" (albeit quite logical) that the same complex can be obtained with the Fe(II) ion.

Other more subtle considerations involved the evaluation of the ligand-field trends based on the ligand's π-accepting and π-donating ability. For example, it is generally agreed that 2,2′-bipyridine (bpy) and 1,10-phenantroline (phen) act as π-acceptors that lower the energy of the metal's t_{2g} orbitals, thus increasing the ligand-field splitting. Indeed, their tris-homoleptic complexes, such as $[Fe(phen)_3]Cl_2$,[7] are found almost exclusively in the LS state. In contrast, the tris-homoleptic Fe(II) complexes of 2,2′-biimidazole (bim), such as $[Fe(bim)_3](SO_4)$,[8] are always found in the HS state, due to the weaker π-accepting ability of the five-member rings in the bim ligand. Nevertheless, the complex $[Fe(bimz)_3](ClO_4)_2$ (bimz = 2,2′-bis-2-imidazoline, which has less extensive π-conjugated system than that of bim) exhibits SCO, which was explained by the more concentrated π-system of the ligand that helps to strengthen the metal–ligand interaction.[9]

Received: March 1, 2017
Published: April 12, 2017

DOI: 10.1021/jacs.7b02098
J. Am. Chem. Soc. 2017, 139, 6437–6447

One should realize, however, that these sometimes vague explanations of the ligand-field strength are generally provided after the magnetic behavior of the particular complex has been already established. Thus, they become justifications that carry a limited predictive power and sometimes contradict other related examples. Herein we suggest a very simple rule for the prediction of the spin state for a specific and widespread series of compounds:

The spin state of Fe(II) complexes that bear a set of three bidentate diimines is determined by the chelating N−N distance *in the noncoordinated ligand*. Complexes with d(N−N) < 2.78 Å and d(N−N) > 2.93 Å adopt the LS and HS states, respectively, while complexes with 2.78 Å < d(N−N) < 2.93 Å exhibit SCO.

We base our reasoning on the ability of a particular ligand to conform to the geometrical requirements of the LS and/or HS state of the Fe(II) ion. By analyzing a wealth of structural data, we demonstrate that this approach results in a reliable prediction of LS, HS, or SCO behavior of the homoleptic complexes with diimines. Finally, we use this simple concept to predict the spin states of three new Fe(II) complexes that have been subsequently prepared and shown to follow the predicted behavior.

RESULTS AND DISCUSSION

Known Homoleptic Fe(II) Complexes with bpy-/phen-Based Ligands. A transition from the LS state to the HS state of an Fe(II) complex is accompanied by a significant increase in the Fe−N bond lengths due to the population of antibonding e_g orbitals in the HS state. The typical Fe−N bond lengths for the LS and HS complexes are in the range of 1.95−2.00 Å and 2.15−2.20 Å, respectively.[10] Therefore, the bond-length analysis is a convenient way to assess the spin state of a particular Fe(II) complex. A search of the Cambridge Structural Database (CSD) revealed ~600 structures of mononuclear complexes in which the six-coordinate Fe(II) ion was surrounded by three identical diimine ligands (or ligand arms) that form five-member chelating rings. The histogram showing the range of the Fe−N bond lengths in these complexes, together with the N−N distance between the chelating N atoms, is presented in Figure 1a. A bimodal distribution of the bond lengths can be seen clearly, with the corresponding average d(Fe−N) values of 1.96 and 2.20 Å. This distribution reflects the ability of the d^6 Fe(II) ion to adopt either the LS or the HS electronic configuration, respectively.

Out of this large group of structures, the majority are represented by complexes that contain $[Fe(bpy)_3]^{2+}$, $[Fe(phen)_3]^{2+}$, or related cations formed by the Fe(II) ion and ligands derived from bpy or phen. The analysis of Fe−N bond lengths in these structures shows a tight unimodal distribution centered at 1.98 Å (Figure 1b), a typical bond length for LS Fe(II) complexes. This is not surprising, as both bpy and phen are classified as π-accepting strong-field ligands that stabilize the LS state. The directionality of the σ-donating nitrogen orbitals in these ligands creates a favorable situation for the overlap with the e_g orbitals of the transition metal and effective π-back-bonding from the t_{2g} orbitals of the metal to the π^* orbitals of the ligands, thus allowing the formation of a stable complex at the bond lengths compatible with the LS state. The conversion of any of these complexes to the HS state would cause the elongation of Fe−N distances to ~2.2 Å, but at this distance the orbital overlap would be dramatically compromised, thus making the HS state energetically inaccessible. Granted, the ligand's geometry can also adapt, but the distortion would be too large to conform to the bite angle at the HS Fe(II) center. One can imagine that upon elongation of the Fe−N bonds to ~2.2 Å, the N···N separation in the bpy- or phen-based ligand would have to increase to direct the nitrogen lone pairs closer to the line connecting the atoms if the orbital overlap were to be optimized in the HS state (Scheme 1). The energetic penalty for such a distortion turns out to be too high.

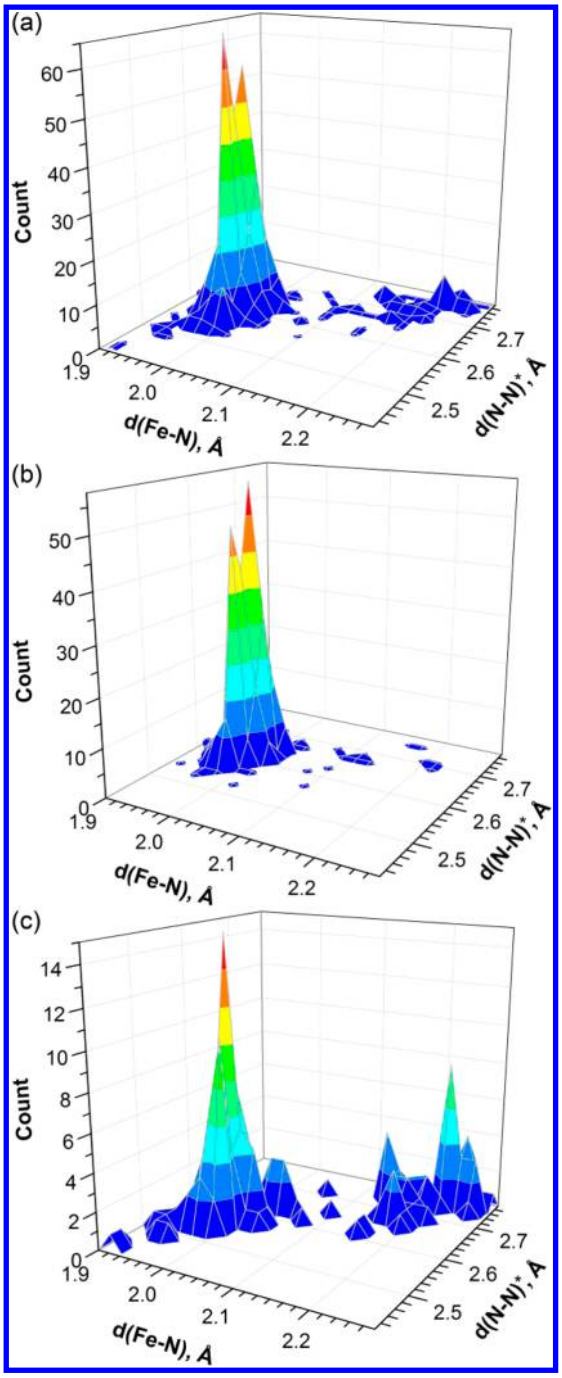

Figure 1. Distribution of Fe−N bond lengths and chelating N−N distances in the crystal structures of tris-homoleptic Fe(II) complexes with diimine ligands (a), with ligands derived from bpy or phen (b), and with diimine ligands not including bpy or phen (c).

Interestingly, a few structures with the bpy/phen-type ligands (Scheme 2) exhibit Fe−N bond lengths in the range of 2.10−

DOI: 10.1021/jacs.7b02098
J. Am. Chem. Soc. 2017, 139, 6437−6447

Scheme 1. Decreasing Fe−N Orbital Overlap upon the LS → HS Transition in the Complex with a bpy-Type Ligand[a]

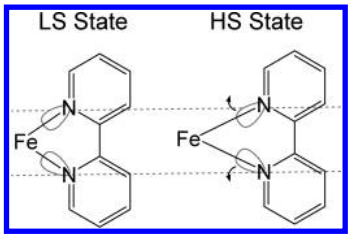

[a]The relative difference in the Fe−N bond lengths between the LS and HS states is exaggerated to make the effect more visible. The arrows indicate the direction in which the bpy ligand has to "open" to optimize the orbital overlap along the Fe−N σ-bonds.

Scheme 2. bpy- or phen-Derived Ligands That Afford HS or SCO Fe(II) Complexes with Tris-homoleptic Coordination Environment

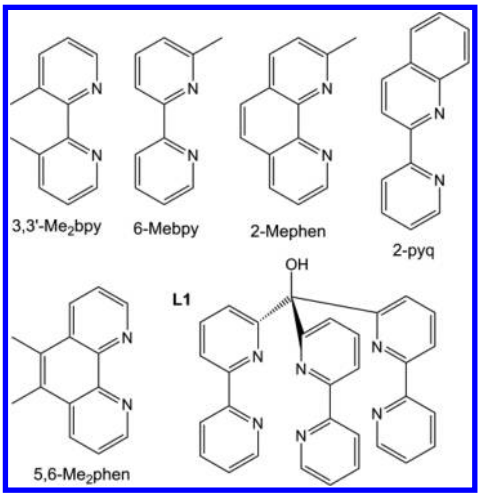

2.20 Å, suggesting the HS state for the corresponding complexes. We now examine these cases, in order to demonstrate that the exceptions can be rationally explained based on the metal−ligand bonding considerations and steric effects.[11] In the structure of $[Fe(3,3'\text{-}Me_2bpy)_3](ClO_4)_2$, the significant steric repulsion between the methyl substituents causes a strong twist of the ligand, resulting in the dihedral angle of 37° between the pyridyl rings. Consequently, the Fe−N bonding is weakened, and the HS state becomes comparable in energy to the LS state; the complex shows SCO behavior.[12] The other type of exceptions stems from the steric hindrance caused by the ligand in the vicinity of the metal center. Complexes $[Fe(6\text{-}Mebpy)_3]$,[13] $[Fe(2\text{-}Mephen)_3]$,[14] and $[Fe(2\text{-}pyq)_3]$[15] contain a methyl substituent or an additional phenylene ring next to the coordinating N atom, thus introducing a substantial crowding in the coordination sphere of the metal ion. Consequently, the Fe−N distances elongate to relieve the steric repulsion, and the complexes adopt the HS state (with L = 2-Mephen) or demonstrate SCO behavior (with L = 6-Mebpy or 2-pyq). Finally, the third type of exceptions deals with the strain introduced by binding chelating diimine ligands that are connected into a more rigid molecular structure, as can be seen for ligand **L1** in Scheme 2. The Fe(II) coordination in the complex $[Fe(\mathbf{L1})](ClO_4)_2$ is strongly distorted from the octahedral geometry, causing the destabilization of the LS state relative to the HS state, which is experimentally observed.[16]

5,6-Me_2phen is the only ligand in Scheme 2 that should not induce any additional structural strain at the metal center. Therefore, the reported crystal structure of $[Fe(5,6\text{-}Me_2phen)_3](ClO_4)_2$, with the average Fe−N distance of 2.120 Å at 100 K,[17] appears dubious, as it suggests the occurrence of SCO for the Fe(II) ion. We synthesized this complex and redetermined its crystal structure. The average Fe−N bond length was found to be 1.972(2) Å at 230 K, unambiguously proving the LS state for this complex. In addition, we did not observe any spin-state change in the magnetic measurements performed from 2 to 400 K (Figure S1). These findings also agree with the reported LS structure of $[Fe(5,6\text{-}Me_2phen)_3][C(CN)_3]_2$ that shows $d(Fe-N)_{av}$ = 1.963 Å.[18]

Known Homoleptic Fe(II) Complexes with Other Diimine Ligands. As shown above for the cases of bpy- and phen-type ligands, the LS state of Fe(II) complexes with such ligands remains predictable as long as there is no noticeable steric effect caused, for example, by the presence of pendant substituents next to the metal-binding sites (e.g., 6-Mebpy) or by tethering the tree bidentate chelating moieties to a central atom (e.g., L1). Therefore, we will continue our consideration of homoleptic tris-diimine complexes of the Fe(II) ion by focusing only on those complexes that contain simple chelating diimine ligands (Scheme 3).

The search over the CSD with the aforementioned restriction resulted in 454 tris-homoleptic structures, containing Fe(II)-coordinated diimine ligands summarized in Scheme 3. After excluding the ligands based on bpy and phen, the analysis of bond lengths in 148 remaining crystal structures led to a well-defined bimodal distribution shown in Figure 1c.

From the previous consideration of the orbital overlap and bite angles in the bpy- and phen-containing complexes, it becomes clear that the N−N separation and the lone-pair directionality in certain groups of ligands will be more disposed to the formation of either the LS or the HS state. To that end, we compiled in Table 1 the N−N distances in the free, noncoordinated diimines, as well as the spin state of their tris-homoleptic complexes with the Fe(II) ion as established in the literature. Crystal structures for many of these ligands have been reported. For the cases in which the crystal structures were not available, we used MP2-level theory to optimize the structure of the ligand and extract the N−N distances. A comparison of calculated and experimental results for several cases in Table 1 shows that such approach is valid.

Experimental crystal structures of some of the ligands shown in Scheme 3, or their derivatives, could be found with the N-donor sites arranged in the syn fashion (Scheme 4a), in which case the determination of the d(N−N) values was straightforward. When the experimental crystal structure was known only with the anti-configuration of the N-donor sites, the distance was calculated as

$$d(\mathrm{N{-}N}) = y - x\cos\alpha - z\cos\beta \quad (1)$$

with the metric parameters defined in Scheme 4b. The same calculation was used in the cases when the ligand's molecular structure could not be optimized to an in-plane arrangement of the N-donor sites in the syn-configuration.[74]

An examination of the data compiled in Table 1 reveals that the ligands with short d(N−N) in the noncoordinated form tend to result in LS Fe(II) tris-diimine complexes, while the

DOI: 10.1021/jacs.7b02098
J. Am. Chem. Soc. 2017, 139, 6437−6447

Scheme 3. Diimine Ligands Covered in This Work

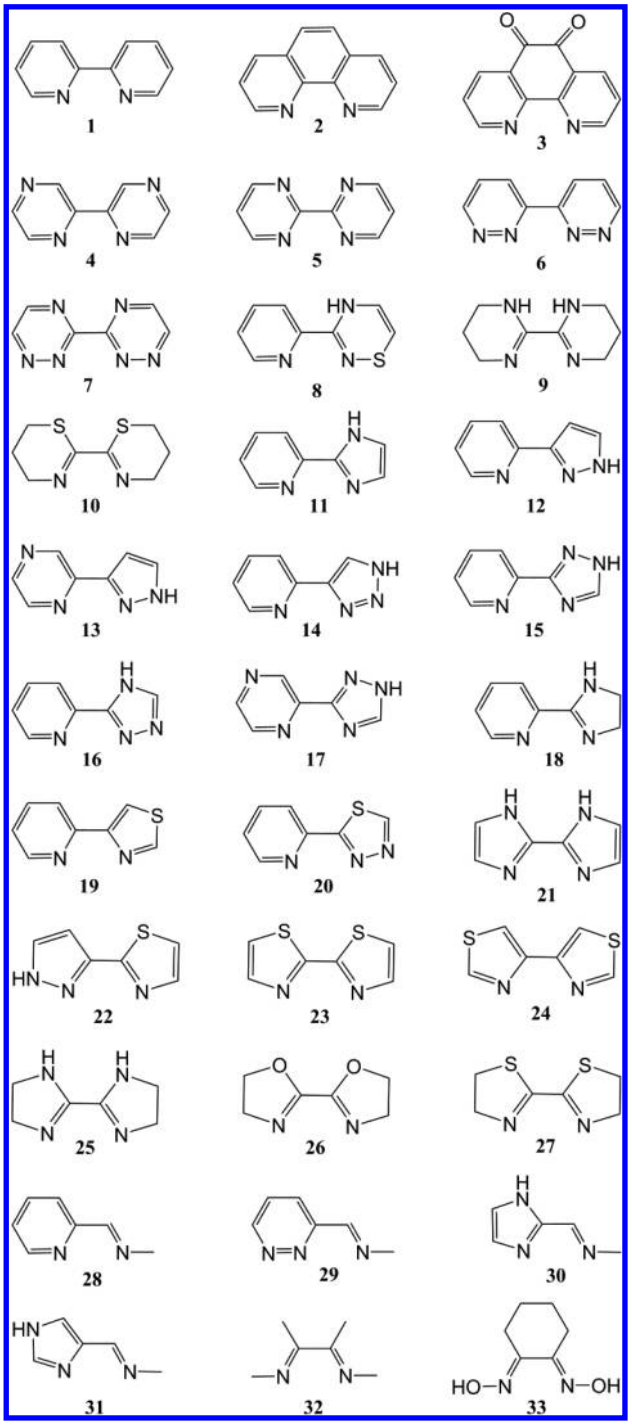

ligands with long d(N−N) favor the HS state. In the case of intermediate N−N distances, SCO behavior is observed. These relations can be explained by the contribution of two factors already considered above in the discussion of bpy- and phen-containing complexes, namely the strain (distortion) imposed on the ligand in the complex and the stability of the Fe−N bonds. We observe that essentially all ligands exhibit a shorter N−N separation in the complex as compared to the value in the free ligand. Moreover, the N−N separation in the LS state is shorter than that in the HS state for the same ligand (Figure 1). These observations indicate that the ligand's structure becomes more strained as it binds to the metal ion. In many

Table 1. N−N Distances in the Free Ligands and the Spin State of Their Tris-homoleptic Fe(II) Complexes

	d(N−N), Å[a]		
ligand	expt[b]	calcd	Fe^{II} spin state
1	*2.692*[19]	*2.695*	LS[20]
2	*2.724*[21]	*2.747*	LS[22]
3	*2.713*[23]	*2.719*	LS[24]
4	*2.722*[25]	*2.714*	LS[26]
5	*2.711*[27]	*2.716*	LS[28]
6	n/a	*2.672*	LS[29]
7[c]	*2.688*[30]	*2.708*	LS[31]
8[c]	*2.682*[32]	*2.708*	LS[32]
9	n/a	*2.746*	SCO[33]
10	*2.672*[34]	*2.650*	LS[35]
11	*2.828*[36]	*2.860*	SCO[37]
12	*2.747*[38]	*2.756*	SCO[39]
13[c]	*2.778*[40]	*2.769*	LS[41]
14	*2.780*[42]	*2.800*	LS[43]
15[c]	2.802[44]	*2.857*	SCO[45]
16[c]	*2.824*[46]	*2.855*	SCO[46,47]
17[c]	*2.843*[48]	*2.869*	SCO[49]
18	*2.784*[50]	*2.791*	SCO[51]
19[c]	*2.758*[52]	*2.766*	LS[53]
20[c]	*2.777*[54]	*2.786*	LS[54]
21	*2.991*[55]	*3.024*	HS[56]
22	*2.847*[39a]	*2.872*	SCO[39a]
23	*2.910*[57]	*2.913*	SCO[57]
24	*2.805*[57]	*2.835*	SCO[57]
25	*2.855*[58]	*2.878*	SCO[9]
26	*2.945*[59]	*2.944*	HS[33a]
27	*2.836*[60]	*2.794*	?[35,d]
28[c]	*2.673*[61]	*2.723*	LS[62]
29[c]	*2.655*[63]	*2.687*	LS[64]
30[c]	*2.882*[65]	3.001	SCO[62,66]
31[c]	*2.867*[67]	*2.955*	SCO[68]
32[c]	*2.652*[69]	*2.658/2.818*[e]	LS,[70] SCO[71,e]
33	2.638[72]	*2.757*	LS[73]

[a]The italicized values were calculated in the anti-arrangement of the N-donor sites, according to eq 1 and Scheme 4. [b]Average distances were taken in the cases when more than one ligand molecule was present in the asymmetric unit. [c]If unsubstituted ligand could not be found, an experimental structure that would have the least structural distortion caused by the substitution was used, and the d(N−N) in the unsubstituted ligands was calculated for comparison. [d]The complex is LS below room temperature, but the spin state above room temperature was not investigated.[35] [e]The complex is LS-Fe^{II} at low temperature, but at higher temperature an outer-sphere metal-to-ligand electron transfer results in the HS Fe^{II} complex, in which one of the ligands becomes an anionic radical (see the text).[71] The d(N−N) values were calculated for both neutral and anionic forms of **32**, respectively.

Scheme 4. (a) The N−N Distance in the Planar Syn-Form of a Noncoordinated Diimine Ligand. (b) The parameters Used To Calculate the N−N Distance in the Anti-Arrangement of a Noncoordinated Ligand

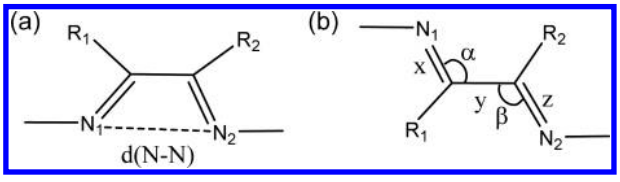

DOI: 10.1021/jacs.7b02098
J. Am. Chem. Soc. 2017, 139, 6437−6447

cases, however, the LS state is still energetically favorable as compared to the HS state, because the strain on the ligand is compensated by the formation of shorter and more stable metal−ligand bonds in the LS complex. Nevertheless, if the d(N−N) value is large, the strain required to form the LS state is too high to be compensated by the more stable metal−ligand bonds. In such a case, the complex favors the HS state. Quite logically, for the intermediate N−N distances, a situation arises when the energies of the LS and HS states become comparable, affording the LS↔HS interconversion (SCO) to be driven by external factors.

The diimine ligands shown in Scheme 3 can be classified in five groups: (i) ligands that combine two six-member rings; (ii) ligands that combine one six-member and one five-member rings; (iii) ligands that combine two five-member rings; (iv) ligands that combine a six- or five-member ring and an open-chain imine; (v) open-chain diimines. As the following discussion will show, the N−N distances in noncoordinated ligands and the spin states of the Fe(II) complexes correlate quite well with this classification.

Ligands with Two Six-Member Rings and Open-Chain Diimine Ligands. Diimine ligands **1**−**10**, formed by two six-member rings, exhibit short d(N−N) values (<2.75 Å). Consequently, their tris-homoleptic Fe(II) complexes exist almost exclusively in the LS state. As can be seen from Table 1, the only exception (not taking into account the complexes with sterically demanding ligands shown in Scheme 2) is provided by complexes of 2,2′-bi-1,4,5,6-tetrahydropyrimidine (**9**). Nelson and co-workers reported that both perchlorate and tetraphenylborate salts of the $[Fe(\mathbf{9})_3]^{2+}$ cation exhibit SCO.[33a] We also note that the d(N−N) value calculated for this ligand is on the higher end of the values observed for ligands **1**−**10**. One could argue that π-accepting ability of **9** is weakened by the loss of aromaticity, which would make it a weaker ligand. Nevertheless, the same argument should hold for 2,2′-bi-4,5-dihydrothiazine (**10**), but its Fe(II) complexes exhibit only the LS state. The substitution of S atoms for the NH groups in **9** leads to a slightly larger size of the six-member rings in **10**, thus pushing the N-donor sites closer and decreasing the bite angle or the chelating pocket. As a result, the salts of $[Fe(\mathbf{10})_3]^{2+}$ with the same anions are LS.[35]

Similar to the first group are open-chain diimine ligands **32** and **33**. Both types of ligands feature similar angles at the N and C atoms of the chelating fragment, which results in similar bite angles and N−N separations. The tris-homoleptic Fe(II) complexes of ligands **32** and **33** are also LS.[70,73,75] A single exception, however, was described to occur in the complex $[Fe(dad)_3][Fe(pda)_2]$ (dad = *N*,*N*′-bis(phenyl)-2,3-dimethyl-1,4-diaza-1,3-butadiene; H_2pda = *N*,*N*′-bis(pentafluorophenyl)-*o*-phenylenediamine).[71] At low temperatures, the tris-homoleptic cation $[Fe^{II}(dad)_3]^{2+}$ exists in the LS state, but above 235 K, outer-sphere electron transfer from the $[Fe^{II}(pda)_2]^{2-}$ anion to the cation causes the latter to adopt a configuration $[Fe^{II}(dad^{\bullet-})(dad)_2]^{+}$, in which the Fe(II) center is HS and one of the dad ligands becomes an anionic radical. Thus, in this unique case the octahedrally coordinated Fe(II) ion undergoes an unusual SCO, due to the change in the electronic structure of one of the coordinated ligands. Interestingly, the theoretically optimized structure of the uncoordinated $dad^{\bullet-}$ revealed the N−N distance of 2.818 Å, which is substantially longer than the value of 2.658 Å observed for the neutral ligand. As will be shown below, this longer d(N−N) value falls in the range for which the SCO in the tris-homoleptic Fe(II) complexes can be expected.

Ligands with One Six-Member and One Five-Member Ring. When a six-member ring is replaced by a five-member one (ligands **11**−**20**), the N−N distance becomes longer, due to the smaller internal angle of the five-member ring that causes the increase in the outer angle at the N-donor site (α or β in Scheme 4). As a result, a larger strain is imposed on the ligand to decrease the N−N separation and direct the N-donor lone pairs into proper orientation to optimize bonding in the LS state of the complex. Consequently, such ligands tend to increase the stability of the HS state relative to the LS state, in many cases leading to the SCO between these states. The SCO behavior was reported for tris-homoleptic Fe(II) complexes of ligands **11**, **12**, and **15**−**18**, while complexes of ligands **13**, **14**, **19**, and **20** were found only in the LS state.

An examination of the experimental data for ligands **11**−**20** in Table 1 also reveals that the ligands that form SCO Fe(II) complexes generally exhibit larger N−N distances. The value of 2.78 Å appears to be critical, as all ligands in which the N−N separation exceeds this value furnish SCO Fe(II) complexes (Figure 2). The only exception is given by ligand **12**, which

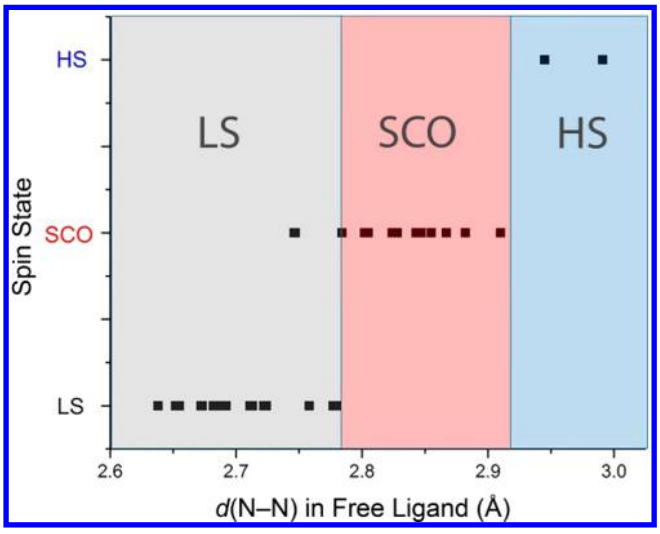

Figure 2. A correlation diagram for predicting the spin state of homoleptic tris-diimine Fe(II) complexes depending on the experimental N−N separation in the free diimine ligands. (A similar diagram for the theoretically calculated d(N−N) values is provided in the Supporting Information, Figure S2).

forms SCO complexes[39] even though d(N−N) = 2.747 Å. An illustrative comparison can be made between ligands **16** and **20**, which differ by the presence of the NH group or S atom, respectively, in the five-member ring. The introduction of the larger S atom effectively decreases the bond angle (α or β in Scheme 4) at the chelating N-donor site of the five-member ring, from 127.5° in **16** to 123.3° in **20**, pushing it closer to the N-donor site on the six-member ring and favoring the LS state over the HS state in the Fe(II) complex. As a result, $[Fe(\mathbf{16})_3]^{2+}$ exhibits SCO[46,47] while $[Fe(\mathbf{20})_3]^{2+}$ exists only in the LS state.[54]

Ligands with Two Five-Member Rings. Diimine ligands formed by two five-member rings show even larger N−N separations, in some cases close to 3.0 Å (Table 1). Consequently, an increased strain would be imposed on the ligand in the LS structure of the tris-homoleptic Fe(II)

DOI: 10.1021/jacs.7b02098
J. Am. Chem. Soc. 2017, 139, 6437−6447

complex, and the corresponding complexes of ligands **21**–**26** either show SCO or exist only in the HS state. The latter situation was observed for complexes of ligands **21** and **26**, which have d(N–N) above 2.93 Å. The complexes of ligands whose d(N–N) is below this value exhibit SCO (Figure 2).

As was already mentioned, the d(N–N) value can be tuned by the size of the heteroatom in the ring, generally decreasing from the O- to N- to S-containing heterocycles, as the larger heteroatom leads to the smaller outer angle (α or β in Scheme 4) at the chelating N-donor site and the smaller N–N separation. For example, the change from the smaller N atom in **21** to the larger S atom in **23** causes the decrease in d(N–N) from 2.991 to 2.910 Å, which is sufficient to achieve SCO in complexes of the $[Fe(\mathbf{23})_3]^{2+}$ ion,[57] while complexes of the $[Fe(\mathbf{21})_3]^{2+}$ ion are always HS.[76] Another relevant comparison is provided by ligands **26**, **25**, and **27**, which contain O, N, and S heteroatoms and exhibit the d(N–N) values decreasing from 2.945 to 2.855 to 2.836 Å, respectively. As a result, the tris-homoleptic Fe(II) complex with **26** is HS, while the analogous complex with **25** exhibits SCO. Complexes of the $[Fe(\mathbf{27})_3]^{2+}$ ion were reported to be LS at room temperature, but their temperature-dependent behavior was not investigated.[35] We believe that such complexes should exhibit SCO above the room temperature, and their magnetic behavior should be studied more thoroughly.

Ligands with a Five- or Six-Member Ring and an Open-Chain Imine. Ligands **28**–**31** also reflect very well the influence of the N–N distance in the free ligand on the spin state of the tris-homoleptic Fe(II) complex. Ligands **28** and **29**, which contain a six-member ring, behave like ligands with two six-member rings or open-chain diimines, all of which have similar bond angles at the chelating N-donor sites and d(N–N) below 2.78 Å. Consequently, their Fe(II) complexes exist in the LS state.[62,64] Replacing the six-member ring with the five-member ring has the already expected effect: the d(N–N) in ligands **30** and **31** exceeds 2.78 Å and their Fe(II) complexes exhibit SCO.[62,66,68]

Spin-State Prediction. The analysis of the correlation between the N–N separation in the free ligands and the spin state of the corresponding tris-homoleptic Fe(II) complexes (Figure 2) clearly reveals the empirical rule formulated in the beginning of this article. To test the predicting power of this rule, we set out to modify some of the ligands shown in Scheme 3 in order to move the d(N–N) values between the three regions of the correlation diagram. The original ligands and their modified versions, along with the d(N–N) values, are shown in Table 2. The d(N–N) values obtained from the optimized geometries indicate that tethering the noncoordinating side of ligands **1** and **25** with a mono- or diatomic bridge, respectively, leads to the elongated N–N distances in **1a** and **25a**, pushing them into the range characteristic of ligands that form only HS Fe(II) complexes. In contrast, N-alkylation of ligand **21** places its derivative **21a** at the borderline that separates the ligands promoting LS or SCO behavior in the Fe(II) complexes.

We synthesized perchlorate salts of tris-homoleptic Fe(II) complexes with ligands **1a**, **21a**, and **25a** and investigated their crystal structures and magnetic properties. An examination of the Fe–N bond lengths in the crystal structures of $[Fe(\mathbf{1a})_3](ClO_4)_2$ and $[Fe(\mathbf{25a})_3](ClO_4)_2$ determined at 100 and 173 K, respectively, revealed values typical of the HS Fe(II) ion (Table 3). The magnetic measurements showed that both complexes remain in the HS state between 2 and 300 K (Figure 3), thus

Table 2. Changes in the N–N Distances upon Chemical Modification of Some Ligands and the Predicted Spin State for the Tris-homoleptic Fe(II) Complexes of the Modified Ligands

Original Ligand and d(N–N), Å	Observed Fe^{II} Spin State	Modified Ligand and d(N–N), Å[a]	Predicted Fe^{II} Spin State
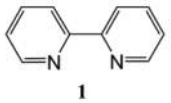 **1** 2.692[19]	LS[20]	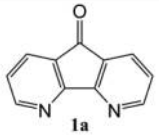 **1a** 3.233	HS
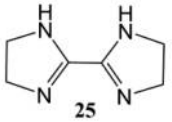 **25** 2.855[58]	SCO[9]	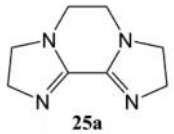 **25a** 3.004	HS
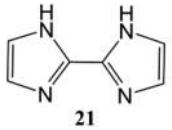 **21** 2.991[55]	HS[76]	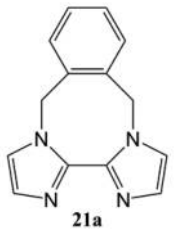 **21a** 2.768	LS or SCO

[a]All values for the modified ligands were obtained by theoretical calculations.

Table 3. Fe–N Bond Lengths in Complexes $[Fe(L)_3](ClO_4)_2$, Where L = 1a, 21a, and 25a

	1a	21a	25a
T, K	173	100	100
d(Fe–N), Å	2.197(4)	1.963(4) (×3)	2.227(2) (×2)
	2.204(4)	1.987(6) (×3)	2.228(2) (×2)
	2.213(3)		2.231(2) (×2)
	2.222(4)		
	2.227(4)		
	2.243(4)		

confirming the prediction based on the d(N–N) values calculated for the free ligands.

In contrast, $[Fe(\mathbf{21a})_3](ClO_4)_2$ showed SCO at rather high temperatures (Figure 3), again in agreement with our prediction. The strain introduced by the eight-member ring in ligand **21a** forces the N-donor sites in the chelating pocket closer to each other. In fact, the d(N–N) value in **21a** decreases dramatically as compared to that in **21** (Table 2), moving slightly below the critical value of 2.78 Å that separates the ligands that promote the LS and SCO behavior. This dramatic change is also reflected in the rather high temperature of SCO in $[Fe(\mathbf{21a})_3](ClO_4)_2$, for which the midpoint of the spin-state conversion is found at $T_{1/2}$ = 302(2) K. The LS→HS conversion itself appears to be gradual and nearly complete around 400 K. The single-crystal X-ray diffraction analysis established that this complex crystallizes in the noncentrosymmetric cubic space group $P2_13$. The Fe–N bond lengths

DOI: 10.1021/jacs.7b02098
J. Am. Chem. Soc. 2017, 139, 6437–6447

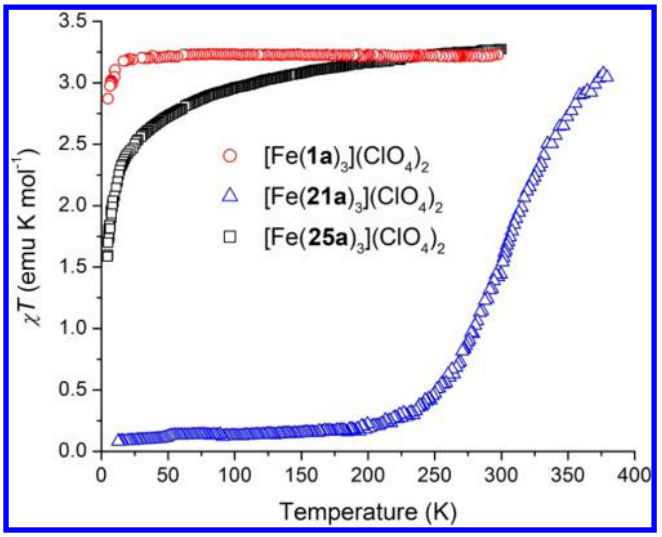

Figure 3. Temperature dependence of χT for $[Fe(L)_3](ClO_4)_2$, where L = **1a** (red), **21a** (blue), and **25a** (black).

determined at 100 K clearly reveal that the Fe(II) center is in the LS state (Table 3).

Such dramatic difference in the magnetic behavior of the SCO complex $[Fe(\mathbf{21a})_3](ClO_4)_2$ vs the HS complex $[Fe(\mathbf{21})_3](BF_4)_2$[56] is difficult to justify by arguments about the changes in the π-accepting/donating ability of the ligands, as one generally would not expect the N-alkylation to alter that ability so strongly. However, considering the change in the orientation of the lone pairs on the N-donor sites and their better arrangement toward the bonding in the LS state in ligand **21a** as compared to ligand **21**, the observed change in the magnetic behavior of the Fe(II) complexes is quite reasonable, keeping in mind the preceding discussions.

Higher-Level Theoretical Analysis. In order to support our somewhat simple approach to the prediction of the spin state of the Fe(II) complexes considered herein, we carried out a more accurate analysis of the spin-state energetics using DFT calculations. The relative stability of the LS and HS states for a particular complex was assessed by evaluating the difference in the zero-point energies of the two states, $\Delta E^\circ_{HL} = E^\circ_{HS} - E^\circ_{LS}$. In DFT, the predicted value of ΔE°_{HL} strongly depends on the functional used, and so far no functional has emerged as the method of choice for accurate determination of this difference.[5] It has been shown, however, that the majority of modern functionals can provide a reliable estimate of the change in the ΔE°_{HL} value as a function of the coordination environment of the metal ion.[77] Hence, following on our previous work, in order to keep the analysis concise, we have performed the calculations using only the standard PBE functional, which is a generalized gradient approximation (GGA) and which as such is expected to overestimate ΔE°_{HL}.

Summarized in Table 4 are the ΔE°_{HL} values calculated with the PBE functional for the tris-homoleptic Fe(II) complexes of ligands that appear in Table 2. The PBE functional severely overstabilizes the LS state, as can be seen from the positive values of ΔE°_{HL} for all six compounds, including complexes with ligands **21**, **1a**, and **25a**, which were found to exist only in the HS state by the magnetic measurements. Nevertheless, the change in the ΔE°_{HL} values in the corresponding ligand pairs, $\Delta(\Delta E^\circ_{HL})$, agrees well with the experimentally observed changes in the magnetic behavior of the complexes. The decrease in ΔE°_{HL}, which indicates the stabilization of the HS state relative to the LS state, is observed upon transition from the complexes containing ligands **1** and **25** to the complexes with ligands **1a** and **25a**, in agreement with the larger N−N separation in the latter ligands. Conversely, the ΔE°_{HL} value increases upon changing ligand **21** to ligand **21a**, which agrees with the decreased stability of the HS state and the observation of the SCO in $[Fe(\mathbf{21a})_3](ClO_4)_2$ as compared to the HS-only behavior of $[Fe(\mathbf{21})_3](ClO_4)_2$.

Table 4. Calculated Values of the HS-LS Zero-Point Energy Difference, ΔE°_{HL}, and Their Variations, $\Delta(\Delta E^\circ_{HL})$, in Tris-homoleptic Fe(II) Complexes of Ligands 1, 1a, 21, 21a, 25, and 25a

ΔE°_{HL}, cm^{-1}		$\Delta(\Delta E^\circ_{HL})$, cm^{-1}
1	**1a**	**1 → 1a**
+11137	+3783	−7354
25	**25a**	**25 → 25a**
+7008	+889	−6119
21	**21a**	**1 → 1a**
+6476	+8081	+1606

CONCLUSIONS

In summary, a comprehensive analysis of the metric parameters in the structures of tris-homoleptic Fe(II) complexes with diimine ligands revealed a strong correlation between the magnetic behavior of the complex and the N−N distance between the chelating N-donor sites in the free ligand. This correlation allowed us to establish a simple empirical rule for the prediction of the spin state of such complexes, namely the d(N−N) values in the range of 2.78−2.93 Å indicate the diimine ligand might be used to achieve spin-crossover behavior in the tris-homoleptic Fe(II) complexes. The shorter or longer N−N separations only lead to the low-spin or high-spin behavior, respectively. The rule was successfully tested by modifying three of the examined ligands in order to force the change in the magnetic behavior of their Fe(II) complexes.

Our analysis conclusively demonstrates that the shorter and longer d(N−N) values in the free ligand lead, respectively, to the stronger and weaker ligand field. We believe that these findings have a broader meaning and can be applied to complexes of transition metals with bidentate chelating ligands in general, for example, to quickly predict possible shifts in the photophysical or electrochemical properties of the complexes.

It is important to note, however, that the spin-crossover behavior in transition metal complexes can sometimes change substantially depending on subtle effects of crystal packing, including the presence of interstitial counterions and solvent molecules. Therefore, the rule devised here should be used with caution and viewed as a guiding principle for evaluating potential changes in the ligand field strength but not as a guaranteed method to predict the spin-crossover behavior.

MATERIALS AND METHODS

Synthesis. All reactions were performed under an N_2 atmosphere using standard Schlenk techniques. The ligands 1,1′-(*α*,*α*′-*o*-xylyl)-2,2′-biszimidazole (**21a**)[78] and 2,3,5,6,8,9-hexahydrodiimidazo[1,2-*a*:2′,1′-*c*]pyrazine (**25a**)[79] were synthesized according to the published procedures. All other starting materials and solvents were purchased from Aldrich and used as received. Anhydrous commercial solvents were additionally purified by passing through a double-stage drying/purification system (Glass Contour Inc.). Elemental analyses were performed by Atlantic Microlab, Inc. (Norcross, GA).

DOI: 10.1021/jacs.7b02098
J. Am. Chem. Soc. 2017, 139, 6437−6447

Table 5. Data Collection and Structure Refinement Parameters for $[Fe(L)_3](ClO_4)_2$, Where L = Me_2bpy, 1a, 21a, and 25a

	$[Fe(Me_2bpy)_3](ClO_4)_2\cdot CH_3CN$	$[Fe(\mathbf{1a})_3](ClO_4)_2\cdot CH_3NO_2$	$[Fe(\mathbf{21a})_3](ClO_4)_2$	$[Fe(\mathbf{25a})_3](ClO_4)_2$
formula	$FeCl_2O_8N_7C_{44}H_{39}$	$FeCl_2O_{13}N_7C_{34}H_{21}$	$FeCl_2O_8N_{12}C_{42}H_{36}$	$FeCl_2O_8N_{12}C_{24}H_{36}$
CCDC number	1535402	1535403	1535404	1535401
T, K	230(2)	173(2)	100(2)	100(2)
formula weight	920.59	862.33	951.48	747.40
space group	$P2_1/c$	$P4_32_12$	$P2_13$	$C2/c$
a, Å	10.6982(5)	12.6281(9)	16.976(2)	23.916(5)
b, Å	30.086(1)	12.6281(9)	16.976(2)	10.099(2)
c, Å	13.1081(6)	44.904(3)	16.976(2)	16.810(3)
α, deg	90	90	90	90
β, deg	103.640(1)	90	90	131.277(2)
γ, deg	90	90	90	90
V, Å^3	4100.1(3)	7161(1)	4892(2)	3051(1)
Z	4	8	4	4
crystal color	red	red	red	red
crystal size, mm^3	0.10 × 0.12 × 0.20	0.31 × 0.35 × 0.41	0.07 × 0.15 × 0.21	0.10 × 0.24 × 0.31
d_{calcd}, g cm^{-3}	1.491	1.600	1.022	1.627
μ, mm^{-1}	0.563	0.649	0.345	0.739
λ, Å	0.71073	0.71073	0.71073	0.71073
θ_{max}, deg	28.52	27.76	26.49	28.49
total reflections	47618	79936	8875	14110
R_{int}	0.034	0.055	0.030	0.044
unique reflections	9790	8383	3343	3633
parameters refined	579	534	167	213
restraints used	0	0	0	0
R_1, wR_2 $[I > 2\sigma(I)]$[a]	0.047, 0.128	0.048, 0.105	0.070, 0.183	0.040, 0.101
R_1, wR_2 (all data)	0.063, 0.144	0.057, 0.109	0.078, 0.190	0.055, 0.111
goodness of fit[b]	1.049	1.130	1.033	1.053
diff peak/hole, e Å^{-3}	0.74, −0.49	0.85, −0.54	0.54, −0.37	0.84, −0.56

[a] $R_1 = \Sigma||F_0| - |F_c||/\Sigma|F_0|$; $wR_2 = [\sum[w(F_0^2 - F_c^2)^2]/\Sigma[w(F_0^2)^2]]^{1/2}$. [b] Goodness-of-fit = $[\sum[w(F_0^2 - F_c^2)^2]/(N_{obs} - N_{params})]^{1/2}$, based on all data.

Caution! The complexes between metal ions and organic ligands with perchlorate counterion are potentially explosive. The compounds should be prepared in small amounts and handled with great care!

$[Fe(5,6\text{-}Me_2phen)_3](ClO_4)_2\cdot CH_3CN$. A 36.2 mg (0.10 mmol) amount of $Fe(ClO_4)_2\cdot 6H_2O$ and 62.4 mg (0.30 mmol) of 5,6-Me_2phen were placed in a 25 mL Schlenk tube. After 7.0 mL of anhydrous acetonitrile was added, the mixture was stirred for 30 min, affording a dark-red solution, which was filtered and layered with 10 mL of diethyl ether. The red crystals that formed after several days were washed successively with methanol and diethyl ether and dried by suction. Yield = 61.0 mg (66%).

$[Fe(\mathbf{1a})_3](ClO_4)_2\cdot MeNO_2$. A 36.2 mg (0.10 mmol) amount of $Fe(ClO_4)_2\cdot 6H_2O$ and 54.6 mg (0.30 mmol) of 4,5-diazafluoren-9-one (**1a**) were placed in a 25 mL Schlenk tube. After 8.0 mL of anhydrous nitromethane was added, the mixture was stirred for 10 min, affording an orange-red solution, which was filtered and left in the N_2-filled glovebox for slow evaporation. The red cubic-shaped crystals that formed after several days were washed successively with ethanol and diethyl ether and dried by suction. Yield = 52.6 mg (61%). Anal. Calcd. (found) for $FeCl_2O_{13}N_7C_{34}H_{21}$: C, 47.36 (47.82); H, 2.45 (2.52); N, 11.37 (11.49).

$[Fe(\mathbf{21a})_3](ClO_4)_2$. A 18.1 mg (0.05 mmol) amount of $Fe(ClO_4)_2\cdot 6H_2O$ and 35.4 mg (0.15 mmol) of **21a** were placed into different sides of a 6 mL H-shaped tube. Anhydrous methanol was carefully added until the solutions from both sides of the H-tube connected (~6 mL of methanol). The tube was left under N_2 atmosphere. The red crystals that formed after 2 weeks were washed successively by ethanol and diethyl ether and dried by suction. Yield = 38.1 mg (79%). Anal. Calcd (found) for $FeCl_2O_8N_{12}C_{42}H_{36}$: C, 52.35 (52.13); H, 3.77 (3.92); N, 17.44 (17.35).

$[Fe(\mathbf{25a})_3](ClO_4)_2$. A 72.6 mg (0.20 mmol) amount of $Fe(ClO_4)_2\cdot 6H_2O$ and 94.8 mg (0.60 mmol) of **25a** were placed in a 25 mL Schlenk tube. After 6.0 mL of anhydrous acetonitrile was added, the mixture was stirred for 30 min, affording a dark-red solution, which was filtered and layered with 12 mL of diethyl ether. The red crystals that formed after several days were washed successively with methanol and diethyl ether and dried by suction. Yield = 75.0 mg (50%). Anal. Calcd (found) for $FeCl_2O_8N_{12}C_{24}H_{36}$: C, 38.57 (38.14); H, 4.86 (4.83); N, 22.49 (22.20).

Single-Crystal X-ray Diffraction. In a typical experiment, a selected single crystal was suspended in Paratone-N oil (Hampton Research) and mounted on a cryoloop which was placed on a goniometer stage of a Bruker AXS SMART diffractometer equipped with an APEX-II CCD detector. The data sets were recorded as ω-scans in steps of 0.3°. After integration of the data,[80] a multiscan absorption correction was applied.[81] The space group was determined from the analysis of systematic absences.[82] The solution and refinement of the crystal structures were carried out using the SHELX programs.[83] The final refinement was performed with anisotropic atomic displacement parameters for all non-hydrogen atoms, except for strongly disordered atoms of anions and solvent molecules. All H atoms were placed in calculated positions. In the structure of $[Fe(\mathbf{21a})_3](ClO_4)_2$, the ClO_4^- counterions and possible interstitial solvent molecules were severely disordered, which necessitated the use of the SQUEEZE procedure[84] to account for the electron density of the disordered part. The total number of electrons established by the SQUEEZE method was 740 per unit cell, which gave a tentative formula $[Fe(\mathbf{21a})_3](ClO_4)_2\cdot 4MeOH$. A summary of pertinent information relating to unit cell parameters, data collection, and refinements is provided in Table 5.

Magnetic Measurements. The DC magnetic susceptibility was measured on polycrystalline samples using a superconducting quantum interference device (SQUID) magnetometer (Quantum Design MPMS-XL). Measurements were performed between 370 and 1.8 K, with the cooling rate of 1 K/min, under 0.1 T applied field.

DOI: 10.1021/jacs.7b02098
J. Am. Chem. Soc. 2017, 139, 6437−6447

Quantum−Chemical Calculations. The molecular structures of the diimine ligands were optimized by MP2 calculations using Gaussian 09 package with the DG-DZVP basis set. The geometries of selected tris-homoleptic Fe(II) complexes in the LS and HS states were optimized at the DFT level of theory, with the Amsterdam Density Functional (ADF) package.[85] The PBE functional[86] augmented with the D3BJ semiempirical dispersion correction[87] (PBE-D3BJ) was employed in combination with the Slater-type orbital (STO) TZP basis set of triple-ζ polarized quality from the ADF STO basis set database. During the calculations, the atomic core orbitals were kept frozen up to the 1s level for the C and N atoms and up to the 2p level for the Fe atom. Scalar relativistic effects were included by performing the calculations within the zero-order regular approximation (ZORA) for relativistic effects.[88] The optimizations were carried out with no symmetry constraints. The vibrational analyses performed after the geometry optimizations indicated that the located extrema correspond all to true minima (no imaginary frequencies). The Fe−N and N−N distances within the five-member chelate rings were in good agreement with the results of the single-crystal X-ray diffraction analysis (Table S1).

■ ASSOCIATED CONTENT

Supporting Information

The Supporting Information is available free of charge on the ACS Publications website at DOI: 10.1021/jacs.7b02098.

An additional correlation diagram for predicting the spin state of homoleptic Fe(II) tris-diimine complexes and a table of average interatomic distances in the LS and HS optimized geometries of the homoleptic Fe(II) complexes with **1a**, **21a**, and **25a** (PDF)

CIF data for $[Fe(Me_2bpy)_3](ClO_4)_2 \cdot CH_3CN$ (CIF)

CIF data for $[Fe(\mathbf{1a})_3](ClO_4)_2 \cdot CH_3NO_2$ (CIF)

CIF data for $[Fe(\mathbf{21a})_3](ClO_4)_2$ (CIF)

CIF data for $[Fe(\mathbf{25a})_3](ClO_4)_2$ (CIF)

■ AUTHOR INFORMATION

Corresponding Author

*shatruk@chem.fsu.edu

ORCID

Latévi M. Lawson Daku: 0000-0003-1305-6807

Michael Shatruk: 0000-0002-2883-4694

Present Address

‖Department of Chemistry, National University of Singapore, 3 Science Drive 3, Singapore 117543, Singapore.

Author Contributions

The manuscript was written through contributions of all authors. All authors have given approval to the final version of the manuscript.

Notes

The authors declare no competing financial interest.

■ ACKNOWLEDGMENTS

The National Science Foundation is gratefully acknowledged for the support of this research via the Award CHE-1464955 to M.S. The theoretical part of this work was supported by allocation of computing time from the Center for Advanced Modeling Science (CADMOS) at University of Geneva and the High-Performance Computing (HPC) cluster at Florida State University. The authors thank Prof. Andreas Hauser for fruitful discussions.

■ REFERENCES

(1) Murray, K. S. In *Spin-Crossover Materials: Properties and Applications*; Halcrow, M. A., Ed.; John Wiley & Sons Ltd.: New York, 2013; pp 1−54.

(2) Gütlich, P.; Goodwin, H. A. *Top. Curr. Chem.* **2004**, *233*, 1−47.

(3) (a) Goodwin, H. A. *Top. Curr. Chem.* **2004**, *233*, 59−90. (b) Halcrow, M. A. *Polyhedron* **2007**, *26*, 3523−3576.

(4) (a) Hauser, A. *Top. Curr. Chem.* **2004**, *233*, 49−58. (b) Hauser, A. *Top. Curr. Chem.* **2004**, *234*, 155−198.

(5) (a) Ye, S. F.; Neese, F. *Inorg. Chem.* **2010**, *49*, 772−774. (b) Lawson Daku, L. M.; Aquilante, F.; Robinson, T. W.; Hauser, A. *J. Chem. Theory Comput.* **2012**, *8*, 4216−4231. (c) Kepp, K. P. *Coord. Chem. Rev.* **2013**, *257*, 196−209. (d) Costas, M.; Harvey, J. N. *Nat. Chem.* **2013**, *5*, 7−9. (e) Deeth, R. J.; Handley, C. M.; Houghton, B. J. In *Spin-Crossover Materials: Properties and Applications*; Halcrow, M. A., Ed.; John Wiley & Sons Ltd.: New York, 2013; pp 443−454. (f) Paulsen, H.; Schünemann, V.; Wolny, J. A. *Eur. J. Inorg. Chem.* **2013**, *2013*, 628−641. (g) Borgogno, A.; Rastrelli, F.; Bagno, A. *Dalton Trans.* **2014**, *43*, 9486−9496. (h) Houghton, B. J.; Deeth, R. J. *Eur. J. Inorg. Chem.* **2014**, *2014*, 4573−4580. (i) Kepp, K. P. *Inorg. Chem.* **2016**, *55*, 2717−2727. (j) Salomon, O.; Reiher, M.; Hess, B. A. *J. Chem. Phys.* **2002**, *117*, 4729−4737. (k) Jensen, K. P.; Cirera, J. *J. Phys. Chem. A* **2009**, *113*, 10033−10039. (l) Pierloot, K.; Phung, Q. M.; Domingo, A. *J. Chem. Theory Comput.* **2017**, *13*, 537−553.

(6) Robinson, M. A.; Busch, D. H.; Curry, J. D. *Inorg. Chem.* **1963**, *2*, 1178−1181.

(7) DelaVarga, M.; Petz, W.; Neumuller, B.; Costa, R. *Inorg. Chem.* **2006**, *45*, 9053−9063.

(8) (a) Tan, Y.-H.; Wu, J.-J.; Zhou, H.-Y.; Yang, L.-F.; Ye, B.-H. *CrystEngComm* **2012**, *14*, 8117−8123. (b) Jin, Q.; Zhou, L.; Dai, Y.; Xu, L. *Huaxue Xuebao* **2010**, *68*, 149−156.

(9) König, E.; Ritter, G.; Kulshreshtha, S. K.; Nelson, S. M. *Inorg. Chem.* **1982**, *21*, 3022−3029.

(10) Guionneau, P.; Marchivie, M.; Bravic, G.; Létard, J. F.; Chasseau, D. *Top. Curr. Chem.* **2004**, *234*, 97−128.

(11) By steric effects we mean only those that affect the coordination geometry around the metal center.

(12) Craig, D. C.; Goodwin, H. A.; Onggo, D. *Aust. J. Chem.* **1988**, *41*, 1157−1169.

(13) Onggo, D.; Hook, J. M.; Rae, A. D.; Goodwin, H. A. *Inorg. Chim. Acta* **1990**, *173*, 19−30.

(14) Goodwin, H. A.; Kucharski, S. E.; White, H. A. *Aust. J. Chem.* **1983**, *36*, 1115−1124.

(15) Onggo, D.; Hook, J.; Rae, A.; Goodwin, H. *Inorg. Chim. Acta* **1990**, *173*, 19−30.

(16) Knight, J. C.; Alvarez, S.; Amoroso, A. J.; Edwards, P. G.; Singh, N. *Dalton Trans.* **2010**, *39*, 3870−3883.

(17) Ramakrishnan, S.; Suresh, E.; Riyasdeen, A.; Akbarsha, M. A.; Palaniandavar, M. *Dalton Trans.* **2011**, *40*, 3524−3536.

(18) Váhovská, L.; Potocnák, I. *Acta Crystallogr., Sect. E: Struct. Rep. Online* **2012**, *68*, m1524−m1525.

(19) Merritt, L. L., Jr.; Schroeder, E. D. *Acta Crystallogr.* **1956**, *9*, 801−804.

(20) Low, K. S.; Cole, J. M.; Zhou, X.; Yufa, N. *Acta Crystallogr., Sect. B: Struct. Sci.* **2012**, *68*, 137−149.

(21) Nishigaki, S.; Yoshioka, H.; Nakatsu, K. *Acta Crystallogr., Sect. B: Struct. Crystallogr. Cryst. Chem.* **1978**, *B34*, 875−879.

(22) Hoshina, G.; Ohba, S.; Tsuchiya, N.; Isobe, T.; Senna, M. *Acta Crystallogr., Sect. C: Cryst. Struct. Commun.* **2000**, *C56*, e191−e192.

(23) Calderazzo, F.; Marchetti, F.; Pampaloni, G.; Passarelli, V. *J. Chem. Soc., Dalton Trans.* **1999**, 4389−4396.

(24) Gaspar, A. B.; Muñoz, M. C.; Real, J. A. *Compt. Rend.* **2001**, *4*, 193−196.

(25) Blake, A. J.; Champness, N. R.; Cooke, P. A.; Nicolson, J. E. B.; Wilson, C. *Dalton* **2000**, 3811−3819.

(26) Toma, L. M.; Eller, C.; Rillema, D. P.; Ruiz-Pérez, C.; Julve, M. *Inorg. Chim. Acta* **2004**, *357*, 2609−2614.

(27) Fernholt, L.; Rømming, C.; Samdal, S.; et al. *Acta Chem. Scand.* **1981**, *A35*, 707−715.

DOI: 10.1021/jacs.7b02098
J. Am. Chem. Soc. 2017, 139, 6437−6447

(28) Van Albada, G. A.; Smeets, W. J. J.; Spek, A. L.; Reedijk, J. *J. Chem. Crystallogr.* **2000**, *30*, 441−444.
(29) Onggo, D.; Rae, A. D.; Goodwin, H. A. *Inorg. Chim. Acta* **1990**, *178*, 151−163.
(30) Wolińska, E.; Karczmarzyk, Z.; Rykowski, A.; Wysocki, W. *Acta Crystallogr., Sect. E: Struct. Rep. Online* **2011**, *67*, o1613.
(31) Breu, J.; Range, K. J.; Herdtweck, E. *Monatsh. Chem.* **1994**, *125*, 119−140.
(32) Clark, E. R.; Hayward, J. J.; Leontowicz, B. J.; Eisler, D. J.; Rawson, J. M. *CrystEngComm* **2014**, *16*, 1755−1762.
(33) (a) Burnett, M. G.; McKee, V.; Nelson, S. M. *J. Chem. Soc., Dalton Trans.* **1981**, 1492−1497. (b) Ni, Z.; Shores, M. P. *J. Am. Chem. Soc.* **2009**, *131*, 32−33.
(34) Huffman, J. C.; Sattelberger, A. P. *Cryst. Struct. Commun.* **1981**, *10*, 1535−1538.
(35) Nelson, J.; Nelson, S. M.; Perry, W. D. *J. Chem. Soc., Dalton Trans.* **1976**, 1282−1289.
(36) Tinant, B.; Decamp, C.; Robert, F.; Garcia, Y. *Z. Kristallogr. - New Cryst. Struct.* **2010**, *225*, 729−732.
(37) Dosser, R. J.; Eilbeck, W. J.; Underhill, A. E.; Edwards, P. R.; Johnson, C. E. *J. Chem. Soc. A* **1969**, *5*, 810−816.
(38) Singh, K.; Long, J. R.; Stavropoulos, P. *J. Am. Chem. Soc.* **1997**, *119*, 2942−2943.
(39) (a) Harimanow, L. S.; Sugiyarto, K. H.; Craig, D. C.; Scudder, M. L.; Goodwin, H. A. *Aust. J. Chem.* **1999**, *52*, 109−122. (b) Shiga, T.; Oshiro, E.; Nakayama, N.; Mitsumoto, K.; Newton, G. N.; Nishikawa, H.; Oshio, H. *Eur. J. Inorg. Chem.* **2013**, *2013*, 781−787.
(40) Steger, S.; Matuszczak, B.; Mereiter, K. *Cambridge Structural Database*, entry codes ILUTAK, ILUTAK01, 2003.
(41) Smithson, R. J.; Kilner, C. A.; Brough, A. R.; Halcrow, M. A. *Polyhedron* **2003**, *22*, 725−733.
(42) Felici, M.; Contreras-Carballada, P.; Vida, Y.; Smits, J. M. M.; Nolte, R. J. M.; De Cola, L.; Williams, R. M.; Feiters, M. C. *Chem. - Eur. J.* **2009**, *15*, 13124−13134.
(43) Niel, V.; Gaspar, A. B.; Muñoz, M. C.; Abarca, B.; Ballesteros, R.; Real, J. A. *Inorg. Chem.* **2003**, *42*, 4782−4788.
(44) Schollmeyer, D. *Cambridge Structural Database*, entry code XAYSIZ, 2000.
(45) (a) Sugiyarto, K. H.; Craig, D. C.; Rae, A. D.; Goodwin, H. A. *Aust. J. Chem.* **1995**, *48*, 35−54. (b) Stassen, A. F.; De Vos, M.; van Koningsbruggen, P. J.; Renz, F.; Ensling, J.; Kooijman, H.; Spek, A. L.; Haasnoot, J. G.; Gutlich, P.; Reedijk, J. *Eur. J. Inorg. Chem.* **2000**, *2000*, 2231−2237.
(46) Kitchen, J. A.; White, N. G.; Gandolfi, C.; Albrecht, M.; Jameson, G. N. L.; Tallon, J. L.; Brooker, S. *Chem. Commun.* **2010**, *46*, 6464−6466.
(47) Kitchen, J. A.; White, N. G.; Boyd, M.; Moubaraki, B.; Murray, K. S.; Boyd, P. D. W.; Brooker, S. *Inorg. Chem.* **2009**, *48*, 6670−6679.
(48) Wei, Q.; Qiao, C.; Xia, Z.; Chen, S. *Synth. Commun.* **2013**, *43*, 3181−3191.
(49) Bradford, F. E.; Connor, L. P.; Kilner, C. A.; Halcrow, M. A. *Polyhedron* **2004**, *23*, 2141−2151.
(50) Kia, R.; Fun, H.-K.; Kargar, H. *Acta Crystallogr., Sect. E: Struct. Rep. Online* **2009**, *65*, o780.
(51) Goodgame, D. M. L.; Machado, A. A. S. C. *J. Chem. Soc. D* **1969**, *0*, 1420−1421.
(52) Crane, J. D.; McLaughlin, A. *Acta Crystallogr., Sect. E: Struct. Rep. Online* **2004**, *60*, o129−o130.
(53) Onggo, D.; Scudder, M. L.; Craig, D. C.; Goodwin, H. A. *Aust. J. Chem.* **2000**, *53*, 153−158.
(54) Huxel, T.; Demeshko, S.; Klingele, J. *Z. Anorg. Allg. Chem.* **2015**, *641*, 1711−1717.
(55) Cromer, D. T.; Ryan, R. R.; Storm, C. B. *Acta Crystallogr., Sect. C: Cryst. Struct. Commun.* **1987**, *C43*, 1435−1437.
(56) Abushamleh, A. S.; Goodwin, H. A. *Aust. J. Chem.* **1979**, *32*, 513−518.
(57) Craig, D. C.; Goodwin, H. A.; Onggo, D.; Rae, A. D. *Aust. J. Chem.* **1988**, *41*, 1625−1644.
(58) Brennan, C. J.; McKee, V. *Acta Crystallogr., Sect. C: Cryst. Struct. Commun.* **1999**, *C55*, 1492−1494.
(59) Jones, M. D.; Paz, F. A. A.; Davies, J. E.; Raja, R.; Duer, M.; Klinowski, J.; Johnson, B. F. G. *Inorg. Chim. Acta* **2004**, *357*, 3351−3359.
(60) Gaspar, A. B.; Muñoz, M. C.; Real, J. A. *Inorg. Chem. Commun.* **2004**, *7*, 815−817.
(61) Pioquinto-Mendoza, J. R.; Rosas-Ortiz, J. A.; Reyes-Martínez, R.; Conelly-Espinosa, P.; Toscano, R. A.; Germán-Acacio, J. M.; Avila-Sorrosa, A.; Baldovino-Pantaleón, O.; Morales-Morales, D. *Inorg. Chim. Acta* **2015**, *438*, 146−152.
(62) Blandamer, M. J.; Burgess, J.; Elvidge, D. L.; Guardado, P.; Hakin, A. W.; Prouse, L. J. S.; Radulovic, S.; Russell, D. R. *Transition Met. Chem.* **1991**, *16*, 82−91.
(63) Dey, S. K.; Abedin, T. S. M.; Dawe, L. N.; Tandon, S. S.; Collins, J. L.; Thompson, L. K.; Postnikov, A. V.; Alam, M. S.; Müller, P. *Inorg. Chem.* **2007**, *46*, 7767−7781.
(64) Lan, Y.; Kennepohl, D. K.; Moubaraki, B.; Murray, K. S.; Cashion, J. D.; Jameson, G. B.; Brooker, S. *Chem. - Eur. J.* **2003**, *9*, 3772−3784.
(65) Li, Z.; Tian, C.; Nie, W.; Borzov, M. V. *Acta Crystallogr., Sect. E: Struct. Rep. Online* **2011**, *67*, o1165−o1166.
(66) Thompson, J. R.; Archer, R. J.; Hawes, C. S.; Ferguson, A.; Wattiaux, A.; Mathonière, C.; Clérac, R.; Kruger, P. E. *Dalton Trans.* **2012**, *41*, 12720−12725.
(67) McGinley, J.; McCann, M.; Ni, K.; Tallon, T.; Kavanagh, K.; Devereux, M.; Ma, X.; McKee, V. *Polyhedron* **2013**, *55*, 169−178.
(68) (a) Fujinami, T.; Nishi, K.; Matsumoto, N.; Iijima, S.; Halcrow, M. A.; Sunatsuki, Y.; Kojima, M. *Dalton Trans.* **2011**, *40*, 12301−12309. (b) Fujinami, T.; Nishi, K.; Hamada, D.; Murakami, K.; Matsumoto, N.; Iijima, S.; Kojima, M.; Sunatsuki, Y. *Inorg. Chem.* **2015**, *54*, 7291−7300.
(69) Kuhn, N.; Steimann, M.; Walker, I. *Z. Naturforsch., B: J. Chem. Sci.* **2000**, *55*, 992−993.
(70) Blandamer, M. J.; Burgess, J.; Fawcett, J.; Guardado, P.; Hubbard, C. D.; Nuttall, S.; Prouse, L. J. S.; Radulovic, S.; Russell, D. R. *Inorg. Chem.* **1992**, *31*, 1383−1389.
(71) Khusniyarov, M. M.; Weuhermüller, T.; Bill, E.; Wieghardt, K. *Angew. Chem., Int. Ed.* **2008**, *47*, 1228−1231.
(72) Croitor, L.; Coropceanu, E. B.; Siminel, A. V.; Kulikova, O.; Zelentsov, V. I.; Datsko, T.; Fonari, M. S. *CrystEngComm* **2012**, *14*, 3750−3758.
(73) Simonov, Y. A.; Dvorkin, A. A.; Batyr, D. G.; Malinovskii, T. I.; Bulgak, I. I.; Ozol, L. D. *Izv. Akad. Nauk Mold. SSR Ser. Biol. Khim. Nauk* **1982**, 53−56.
(74) In principle, the true distance between the N-donor sites in the syn-configuration and the distance projected from the anti-configuration are not equivalent, but this approximation does not break the spin-state prediction rule established in the present work.
(75) Simonov, Y. A.; Dvorkin, A. A.; Malinovskii, T. I.; Bel'skii, V. K.; Bulgak, I. I.; Batyr, D. G.; Ozols, L. *Koord. Khim.* **1985**, *11*, 1554−1558.
(76) Martinez Lorente, M. A.; Dahan, F.; Petrouleas, V.; Bousseksou, A.; Tuchagues, J. P. *Inorg. Chem.* **1995**, *34*, 5346−5357.
(77) Vargas, A.; Krivokapic, I.; Hauser, A.; Lawson Daku, L. M. *Phys. Chem. Chem. Phys.* **2013**, *15*, 3752−3763.
(78) Thummel, R. P.; Goulle, V.; Chen, B. *J. Org. Chem.* **1989**, *54*, 3057−3061.
(79) Weisman, G. R.; Reed, D. P. *J. Org. Chem.* **1996**, *61*, 5186−5187.
(80) *SMART and SAINT*; Bruker AXS Inc.: Madison, WI, 2007.
(81) Sheldrick, G. M. *SADABS*; University of Gottingen: Gottingen, Germany, 1996.
(82) Sheldrick, G. M. *XPREP. Space group determination and reciprocal space plots*; Siemens Analytical X-ray Instruments: Madison, WI, 1991.
(83) Sheldrick, G. M. *Acta Crystallogr., Sect. A* **2008**, *A64*, 112−122.
(84) Van der Sluis, P.; Spek, A. L. *Acta Crystallogr., Sect. A* **1990**, *A46*, 194−201.

DOI: 10.1021/jacs.7b02098
J. Am. Chem. Soc. 2017, 139, 6437−6447

(85) Te Velde, G.; Bickelhaupt, F. M.; Baerends, E. J.; Fonseca Guerra, C.; Van Gisbergen, S. J. A.; Snijders, J. G.; Ziegler, T. *J. Comput. Chem.* **2001**, *22*, 931−967.
(86) Perdew, J. P.; Burke, K.; Ernzerhof, M. *Phys. Rev. Lett.* **1996**, *77*, 3865−3868.
(87) Grimme, S.; Ehrlich, S.; Goerigk, L. *J. Comput. Chem.* **2011**, *32*, 1456−1465.
(88) (a) Heully, J. L.; Lindgren, I.; Lindroth, E.; Lundqvist, S.; Maartensson-Pendrill, A. M. *J. Phys. B* **1986**, *19*, 2799−2815. (b) Chang, C.; Pelissier, M.; Durand, P. *Phys. Scr.* **1986**, *34*, 394−404. (c) van Lenthe, E.; Baerends, E. J.; Snijders, J. G. *J. Chem. Phys.* **1993**, *99*, 4597−4610. (d) Van Lenthe, E.; Van Leeuwen, R.; Baerends, E. J.; Snijders, J. G. *Int. J. Quantum Chem.* **1996**, *57*, 281−293. (e) van Lenthe, E.; Ehlers, A.; Baerends, E.-J. *J. Chem. Phys.* **1999**, *110*, 8943−8953.

DOI: 10.1021/jacs.7b02098
J. Am. Chem. Soc. 2017, 139, 6437−6447